CONEM 2016 CONGRESSO NACIONAL DE ENGENHARIA MECÂNICA
21 - 25 AGOSTO DE 2016 FORTALEZA - CEARÁ
ABCM 40 anos Associação Brasileira de Engenharia e Ciências Mecânicas

EXPLORATORY EXPERIMENTAL EVALUATION OF CRACK GROWTH RESISTANCE PROPERTIES FOR A NICKEL-CHROMIUM GIRTH WELD OF A CLAD LINED PIPE

Vitor Scarabeli Barbosa, scarabeli@usp.br
Diego Felipe Sarzosa Burgos, dsarzosa@usp.br
Claudio Ruggieri, claudio.ruggieri@usp.br

Department of Naval Architecture and Ocean Engineering, Av. Prof. Mello Moraes, 2231 (PNV-EPUSP), São Paulo SP 05508-030, Brazil

Abstract: *This work presents an exploratory experimental investigation of the ductile tearing properties for the girth weld of a typical C-Mn pipe internally clad with a nickel-chromium corrosion resistant alloy (CRA) using crack growth resistance curves (J - Δa curves). Here, the material of the external pipe is an API 5L Grade X65 pipeline steel whereas the inner clad layer is made of ASTM UNS N06625 Alloy 625. Unloading compliance (UC) testing of the pipeline girth welds employed side-grooved, clamped SE(T) specimens with a weld centerline notch to determine the crack growth resistance curves. This exploratory experimental characterization provides additional toughness data which serve to evaluate the effectiveness of current procedures in determining experimentally measured R-curves for this class of material.*

Keywords: *Ductile fracture, crack growth resistance curve, clade lined pipe, girth weld, SE(T) specimen*

1. INTRODUCTION

The continuously growing demand for energy and natural resources has spurred a flurry of exploration and production activities of oil and natural gas in harsher environments, especially in ultra-deep water offshore hydrocarbon reservoirs. The main challenge faced by the oil and gas industry is to ensure more reliable and fail-safe operations and to reduce the risk of catastrophic failure. In particular, structural integrity analysis of pipeline girth weld is essential in the design and operation of submarine risers and flowlines transporting oil and gas. Here, the accurate prediction of ductile fracture behavior become essential in defect assessment procedures of the weldment region, where undetected crack-like defects may potentially compromise the structural integrity.

Fracture mechanics based approaches to describe ductile fracture behavior in structural components rely strongly on crack growth resistance ($J - \Delta a$ or, equivalently, $CTOD - \Delta a$) curves (also termed R-curves), to characterize crack extension followed by crack instability of the material (Hutchinson, 1983; Anderson, 2005); here, either the J-integral or the crack-tip opening displacement ($CTOD$ or δ) describe the intensity of near-tip deformation (Hutchinson, 1983; Anderson, 2005) and Δa is the amount of crack growth. These approaches allow the specification of critical crack sizes based on the predicted growth of crack-like defects under service conditions. Current standardization efforts now underway (Shen and Tyson, 2009a, b; Shen *et al*., 2009; Mathias *et al*., 2013; Cravero and Ruggieri, 2007a, b; Tang *et al*., 2010; Wang *et al*., 2012) advocate the use of single edge notch tension specimens (often termed SE(T) or SENT crack configurations) to measure experimental R-curves more applicable to high pressure piping systems, including girth welds of marine steel risers. The primary motivation to use SE(T) fracture specimens is the strong similarity in crack-tip stress and strain fields which drive the fracture process for both crack configurations (Nyhus *et al*., 2003; Cravero and Ruggieri, 2005; Silva *et al*., 2006; Shen *et al*., 2008). Moreover, further investigations by Park *et al*. (2010) reveal that SE(T) fracture specimens provide larger flaw tolerances and, at the same time, reduce the otherwise excessive conservatism in contrast to the conventional high constraint compact tension (C(T)) or the single-edge notched bend (SE(T)) specimen. However, while now utilized effectively in fracture testing of pipeline girth welds with limited overmatch, strong mismatch between the weld metal and base plate strength potentially affects the macroscopic mechanical behavior of the specimen in terms of its load-displacement response with a potentially strong impact on the crack growth resistance curve. For example, in sour service operation the C-Mn steel pipeline is internally clad or mechanically lined with a corrosion resistant alloy CRA, thereby potentially resulting in pipeline girth welds with weld metal undermatch.

This work presents an exploratory investigation of the ductile tearing properties of the girth weld of a typical C-Mn pipe internally clad with a nickel-chromium corrosion resistant alloy (CRA) using experimentally measured crack growth resistance curves ($J - \Delta a$ curves). Here, the material of the external pipe is an API 5L Grade X65 pipeline steel with a higher yield stress of 520 MPa and relatively low hardening properties whereas the inner clad layer is made of ASTM UNS N06625 Alloy 625 (American Society for Testing and Materials, 2009, 2011a) with yield stress of 423 MPa and higher hardening. The higher mechanical strength and superior resistance to a wide range of corrosive environments derive from a solid-solution-strengthened nickel-chromium alloy which contain elements such as molybdenum and columbium. Testing of the pipeline girth welds employed side-grooved, clamped SE(T) specimens with a weld centerline notch to determine the crack growth resistance curves based upon the unloading compliance (UC) method using a single specimen technique. This exploratory experimental characterization provides additional toughness data which serve to evaluate the effectiveness of current procedures in determining experimentally measured R-curves for this class of material.

2. $J - R$ CURVE ESTIMATION PROCEDURE

2.1. Evaluation of the J – Integral

For convenience, the total J-integral can be split into elastic, J_e, and plastic components, J_p, as

$$J = J_e + J_p = \frac{K_I^2}{E'} + \frac{A_p}{bB_N} \tag{1}$$

where K_I is the elastic stress intensity factor for the cracked configuration, A_p is the plastic area under the load-displacement curve, B_N is the net specimen thickness at the side groove roots, b is the uncracked ligament ($b = W - a$ where W is the width of the cracked configuration and a is the crack length), factor η represents a nondimensional parameter which relates the plastic contribution to the strain energy for the cracked body and J. In writing the first term of Eq. (1), plane-strain conditions are adopted such that $E = E/(1-\nu^2)$ where E and ν are the (longitudinal) elastic modulus and Poisson's ratio, respectively.

A widely used approach which forms the basis of current standards, such as ASTM E1820 (American Society for Testing and Materials, 2011b) to evaluate J with crack extension follows from an incremental procedure which updates J_e and J_p at each partial unloading point, denoted k, during the measurement of the load *vs.* displacement curve illustrated in Fig. 1(a) and described in the form

$$J^k = {J_e}^k + {J_p}^k \tag{2}$$

where the current elastic strain term is simply given by

$${J_e}^k = \left(\frac{K_I^2}{E'}\right)_k \tag{3}$$

Since the area under the actual load-displacement curve for a growing crack differs significantly from the corresponding area for a stationary crack (which the deformation definition of J is based on) (Anderson, 2005; Kanninen and Popelar, 1985) as depicted in Fig. 1(b), the measured load-displacement records must be corrected for crack extension to obtain accurate estimate of J-values with increased crack growth. The plastic term, J_p^k, can then be evaluated by an incremental formulation proposed by Cravero and Ruggieri (2007b) and Zhu *et al*. (2008) which is more applicable to $CMOD$ data in the form

$$J_p^k = \left[J_p^{k-1} + \frac{\eta_{J-CMOD}^{K-1}}{b_{k-1}B_N}\left(A_p^k - A_p^{k-1}\right)\right] \cdot \Gamma_k \tag{4}$$

with Γ_k defined by

$$\Gamma_k = \left[1 - \frac{\gamma_{LLD}^{k-1}}{b_{k-1}}(a_k - a_{k-1})\right] \tag{5}$$

where factor γ_{LLD} is evaluated from

$$\gamma_{LLD} = \left[-1 + \eta_{J-LLD}^{K-1} - \left(\frac{b_{k-1}}{W\eta_{J-LLD}^{K-1}} \frac{d\eta_{J-LLD}^{K-1}}{d(a/W)}\right)\right] \tag{6}$$

The incremental expressions for J_p defined by Eqs. (4) to (6) contain two contributions: one is from the plastic work in terms of $CMOD$ and, hence, η_{J-CMOD} and the other is due to crack growth correction in terms of LLD by means of η_{J-LLD}. While the resulting J-estimation procedure based on $CMOD$ may appear a little more complex, evaluation of the above expressions is also relatively straightforward provided the two geometric factors, η_{J-CMOD} and η_{J-LLD}, are known.

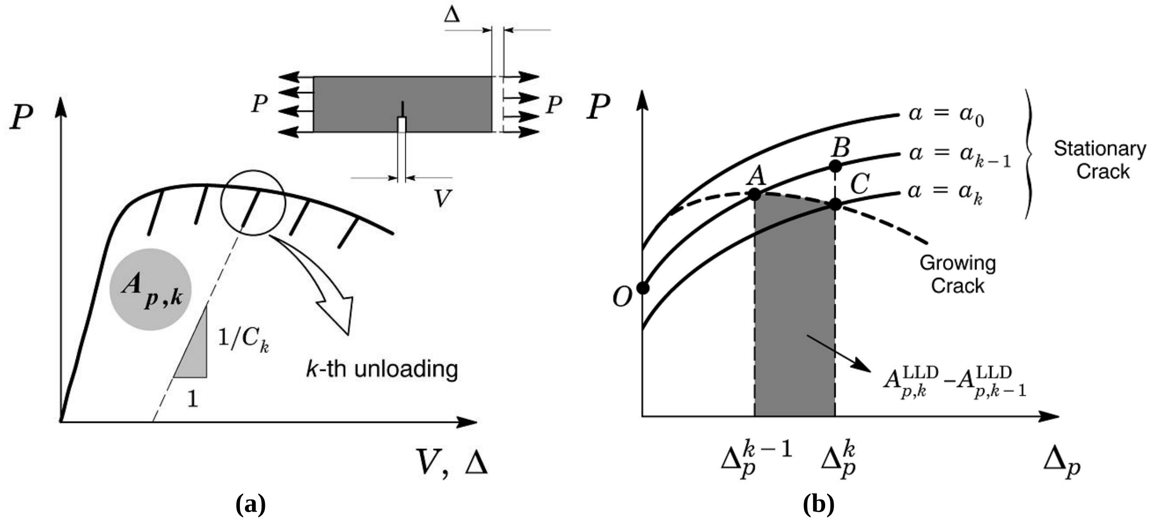

Figure 1: a) Partial unloading during the evolution of load with displacement. b) Load-displacement trajectory for a stationary and growing crack.

2.2. Crack Extension Estimation

Current testing protocols to measure the crack growth resistance response using a single-specimen test are primarily based on the unloading compliance (UC) technique to estimate the (current) crack length from the specimen compliance measured at periodic unloadings with increased deformation. The slope of the load-displacement curve during the $k-th$ unloading depicted in Fig. 1(b) defines the current specimen compliance, denoted C_k ($C = V/P$ where V is the $CMOD$ and P represents the applied load), which depends on specimen geometry and crack length. For the SE(T) crack configurations analyzed here, the specimen compliance based on CMOD is most often defined in terms of a normalized quantity expressed as

$$\mu_{CMOD}^{SET} = \left[1 + \sqrt{Eb_e C_{CMOD}}\right]^{-1} \tag{7}$$

where μ_{CMOD}^{SET}defines the normalized compliances for the SE(T) specimen. In the above expression, E is the longitudinal elastic modulus, and B_e is the effective thickness defined by

$$B_e = B - \frac{(B - B_N)^2}{B} \tag{8}$$

However, the specimen compliance, C, needed to determine the crack length may not reflect changes in specimen geometry due to specimen rotation as the test progresses. In order to correct the tested SE(T) specimen compliance, Shen and Tyson (2009a) equation has been used to correct the specimen rotation.

3. EXPERIMENTAL PROCEDURE

3.1. Material Description and Welding Procedure

The material used in this study was a girth weld of a typical API 5L Grade X65 pipe internally clad with a nickel-chromium corrosion resistant alloy (CRA) made of ASTM UNS N06625 Alloy 625 (American Society for Testing and Materials, 2009, 2011a). The girth weld joint was obtained from a pipe with 203 mm outside diameter and 19 mm wall thickness, t_w = 19 mm, which includes a clad layer thickness, t_c = 3 mm. Girth welding of the pipe was performed in a single V-type groove geometry. The root pass welding was carried out using gas tungsten arc welding process (GTAW) in the 2G (vertical) position in accordance with ASME Boiler and Pressure Vessel Code (2009) Section IX. Subsequently fill passes were carried out using 100% CO_2 gas-shielded flux-cored arc welding (FCAW-G) process in the 5G (horizontal) position. The main FCAW process parameters used for preparation of the welded joint are: i) welding current 200 ~ 250 A; ii) welding voltage 27 ~ 29; iii) average wire feed speed of 11 ~ 12 m/min.

Round tensile specimens having a gage diameter of 6 mm and a gage length of 30 mm were machined parallel to the pipe axis and tested at room temperature to measure the tensile properties of tested materials. The mechanical properties of tensile tests for pipe steel base metal and girth weld metal are set out in Table 1. It can be seen that the yield strength mismatch between pipe steel base metal and weld metal is approximately 25%. Based on Annex F of API 579 (American Petroleum Institute, 2007), the Ramberg-Osgood strain hardening exponents describing the stress-strain response for the base plate and weld metal are estimated as n_{BM} = 18.9 and n_{WM} = 9.7.

Table 1. Material properties of the base plate and weldment for the tested pipeline CRA girth weld.

Base Plate		Weld Metal	
σ_{ys} (MPa)	σ_{ys} (MPa)	σ_{ys} (MPa)	σ_{ys} (MPa)
620	700	462	627

3.2. Specimen Geometry

Unloading compliance (UC) tests at room temperature were performed on center notch weld, clamped SE(T) geometries extracted in the same way as for the round tensile specimens (i.e., from the longitudinal direction of the pipe specimen illustrated in Fig. 2(a)) to measure tearing resistance curves in terms of $J - \Delta a$.

The single edged notched tension specimens were clamped using hydraulic grips with a distance between grips H= $10W$, as illustrated in Fig. 2(b). The initial crack size to thickness ratio (a/W) was set at 0.3. Here, a is the crack depth and W = 16 mm is the specimen width which in turns is equal to the thickness B. It should be emphasized that width is slightly smaller than the pipe thickness, t_w, that ensure transferability of R-curves between SE(T) specimen and pipe. Conducted as part of a collaborative program between the University of São Paulo and Petrobras, testing of these specimens focused on the evaluation of crack growth resistance data for nickel chromium girth welds made in clad lined pipes.

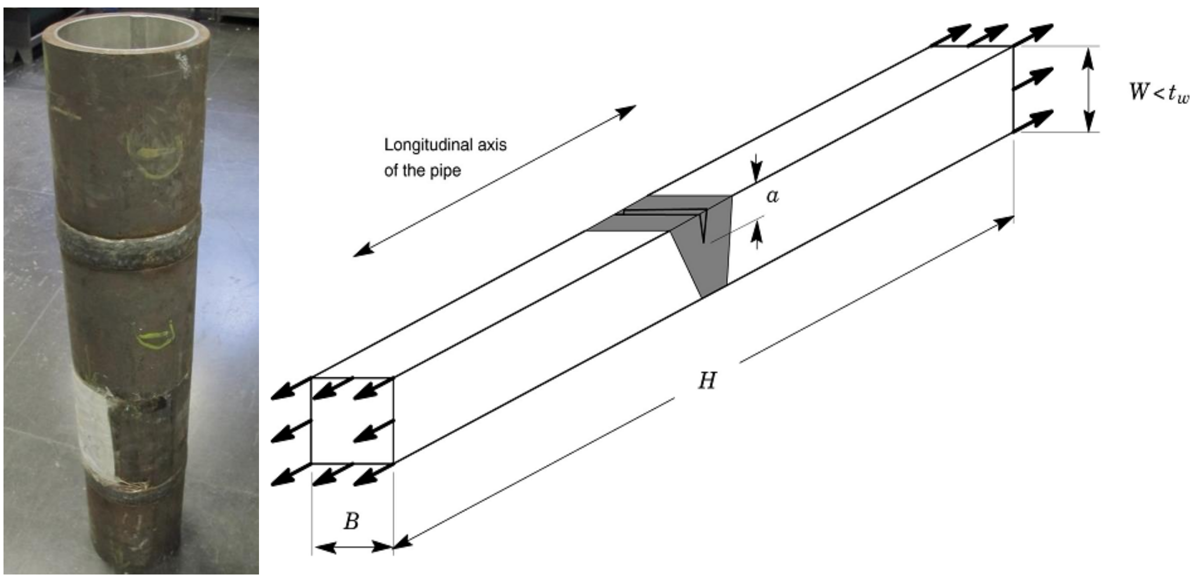

(a) **(b)**

Figure 2: (a) 8-inch pipe (203 mm outer diameter) having overall thickness, t_w = 19 mm and clad layer thickness, t_c = 3 mm; (b) Geometry of tested clamped SE(T) specimen with a/W = 0.3 and H/W = 10 having a weld centerline notch and B x B configuration.

The specimens were precracked in bending using a three-point bend apparatus very similar to a conventional three-point bend test. After fatigue precracking, the specimens were side-grooved to a net thickness of $\sim$85% of the overall thickness (7.5% sidegroove on each side) to promote uniform crack growth and tested following some general guidelines described in Ruggieri and Hippert (2015) and ASTM E1820 (American Society for Testing and Materials, 2011b). Records of load vs. crack mouth opening displacement (CMOD) were obtained for the specimens using a clip gage mounted on knife edges attached to the specimen surface.

4. RESULTS AND DISCUSSION

4.1. J – Resistance Data

The framework for determining J-resistance curves based on $CMOD$ described previously provides the basis for characterizing the ductile fracture response of the tested material. Evaluation of the crack growth resistance curve follows from determining J and Δa at each unloading point of the measured load-displacement data. We follow the work of Mathias *et al*. (2013) and employ all expressions for η_{CMOD} and η_{LLD} applicable to homogeneous materials described in that work, as well as the elastic compliance expressions for clamped SE(T) geometries. Readers are referred to the article of Mathias *et al*. (2013) and references therein for a full account of the $J-R$ curve estimation procedure, including all applicable expressions.

Figure 3 shows a typical load-displacement curve (as described by CMOD) measured from testing the SE(T) specimen with H/W = 10 and a/W = 0.3. Figure 4 shows the measured crack growth resistance curves for the tested SE(T) specimens in which the overall trend of increased J-values with increased amounts of ductile tearing is evident in this plot.

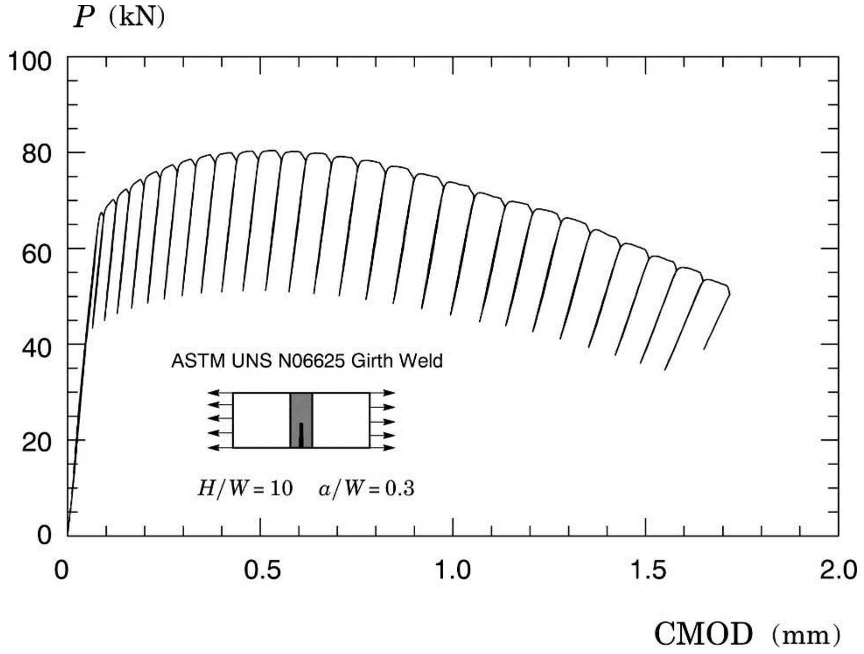

Figure 3: Measured load-$CMOD$ curve for the tested clamped SE(T) specimens with a/W = 0.3.

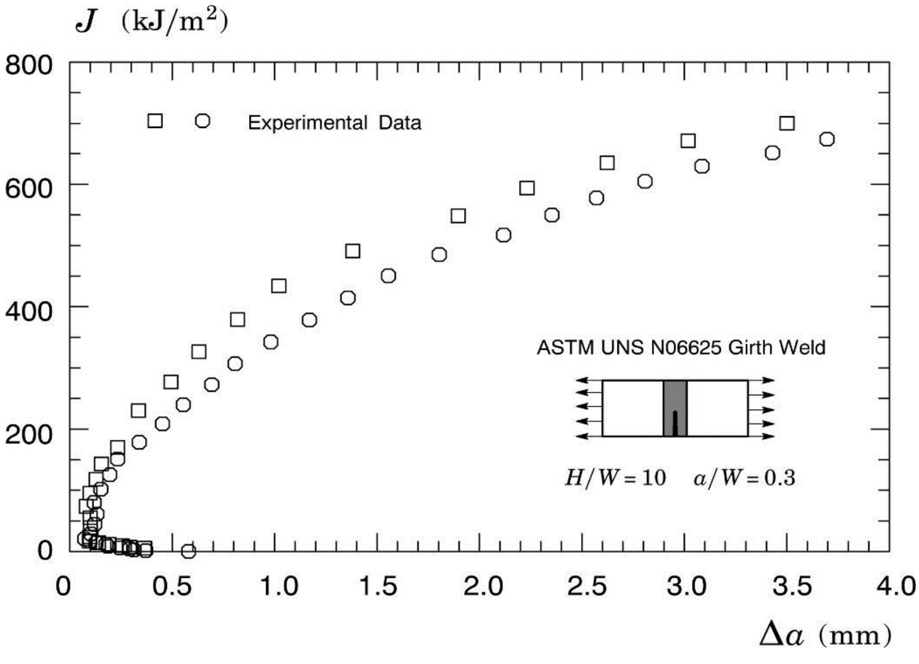

Figure 4: J-resistance curves including crack growth correction for the tested clamped SE(T) specimens.

Further, observe that, despite some inherent scatter in the measured data, the resistance curves show no sign of leveling off in the entire range of ductile tearing thereby typifying a relatively tough material. Overall, the crack growth response derived from the present test procedure appears to be highly describable by the tested SE(T) specimens to serve as a basis for ductile tearing assessments in ECA procedures applicable to clad pipeline girth welds and similar structural components.

Another evident feature in Fig. 4 is the "crack backup" (or apparent negative crack growth) observed in the initial part of the $J-R$ curves for both tested specimens. Despite the rotation correction adopted to evaluate the specimen compliance as briefly described previously, the early compliance measurements display an increase in specimen thickness with increased loading for $0 \leq \Delta a \leq 0.5$ mm. However, such behavior appears to be a recurring feature with this specimen geometry as reported in early works of Joyce *et al.* (1993) and Joyce and Link (1995), and more recently by Drexler *et al.* (2010). While the precise causes of this phenomenon are not yet fully understood, it may be associated with nonstraightness of the crack front after fatigue precracking and large localized deformation at the clamp region early in the test thereby increasing the loading without any measurable increase in $CMOD$. An investigation along this line is progress addressing the potential sources for apparent negative crack growth in fracture testing of the SE(T) geometry.

4.1. Crack Extension Measurements

After testing, all specimens were subjected to heat tinting treatment at high temperatures and then air cooled before being broken apart. A typical crack surface obtained from one of the SE(T) specimens is illustrated in Fig. 5(a). It can be seen that this specimen exhibited a somewhat non-uniform fatigue precrack most likely caused by microstructural heterogeneities at the crack front promoted by the welding process. In order to analyze the fracture surface morphology to identify the primary fracture micromechanism operating during the ductile fracture process, the fracture surface of the SE(T) specimens was observed by a scanning electron microscope (SEM). As can be seen from Fig. 5(b), small inclusions are observed within dimples which imply a ductile fracture mode. Due to crack extension by micro ductile void growth and coalescence, ductile fracture behavior produces a rising resistance curve, at least during the early stages of crack growth (Anderson, 2005; Zhu and Joyce, 2012). Similar features are also observed for the crack surface of the other test specimen.

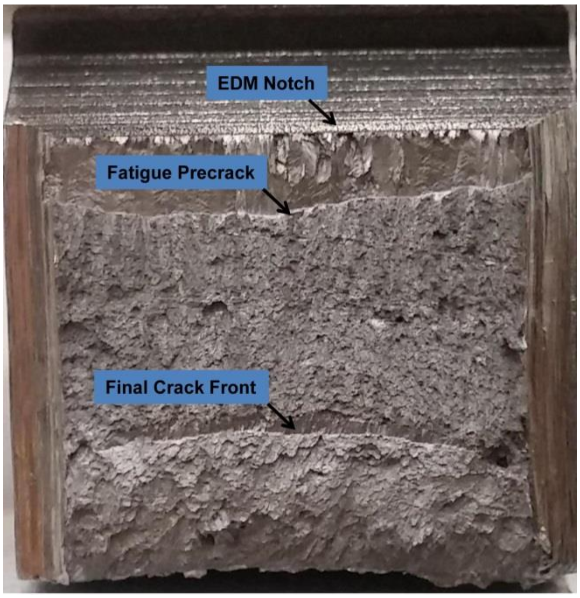

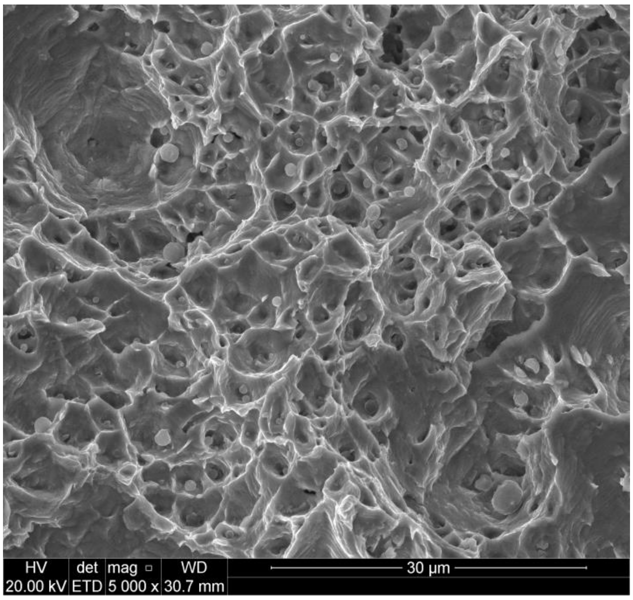

Figure 5: (a) Typical crack surface obtained from one of the tested SE(T) specimens; (b) SEM fractographs of the centre of fracture surface taken from girth weld.

Validation analyses of crack length estimates are also of interest to assess the accuracy of the UC procedure to determine crack growth during the fracture test. Following standard methods based on the 9-point average technique, such as the procedure given by ASTM E1820 (American Society for Testing and Materials, 2011b) and also in Ruggieri and Hippert (2015), the initial and final crack length measured after the test by means of an optical method are compared with crack length estimates derived from the UC method. Table 2 provides the predicted and measured crack extension for all tested fracture specimens in which the deviation between predicted and measured values is defined as $\Lambda = |\Delta a_{measured} - \Delta a_{preditected}|/\Delta a_{measured}$. Surprisingly, the crack extension prediction for one of the tested specimens (CP4) derived from the UC procedure is not in good agreement with the measured amount of ductile tearing; here, the unloading compliance method underestimates the 9-point average crack extension by $\sim 20\%$ thereby plausibly producing an apparent higher J-resistance curve. In contrast, the predicted amount of crack extension for specimen CP5 is in good accord with the measured crack growth and shows a deviation of 5% between the predicted and measured data. While we have not investigated further the cause of the larger deviation between the predicted and measured amount of crack growth for specimen CP4, we argue that the relatively strong, irregular crack front profile could be a plausible reason for the relatively poor agreement between the measured and predicted amount of ductile tearing. Further studies are in progress to investigate these results and to improve the methodology for crack length estimates and crack length measurements.

Table 2: Predicted and measured crack extension for all tested fracture specimens.

Specimen		Measured Post Test (mm)		Compliance Estimation (mm)		Λ(%)
	a_0	a_f	Δa	a_f	Δa	
CP4	5.0	10.5	5.5	9.7	4.3	22
CP5	4.8	10.6	5.8	11.0	6.1	5

4.2. $CTOD$-Resistance Curves

As hinted before, to the extent that J describes the crack-tip conditions with increased crack extension and, further, that a unique $J - CTOD$ relationship holds true for stationary and growing cracks, both $J - \Delta a$ and $CTOD - \Delta a$ curves should characterize equally well the crack growth resistance behavior for the tested material (Hutchinson, 1983; Anderson, 2005). However, because of the widespread use of the $CTOD$ parameter since its introduction in the 70s, when early development conducted at the Welding Institute introduced the concept of a $CTOD$ design curve (Burdekin and Dawes, 1966; Harrison et al., 1979), current defect assessment procedures adopted by the oil and gas industry favor the utilization of $CTOD - R$ curves rather than J-resistance measurements. To facilitate interpretation of the ductile tearing response for the tested nickel-chromium CRA girth weld, we also provide crack growth resistance data in terms of $CTOD - \Delta a$ curves.

Here, we follow the work of Sarzosa *et al.* (2015) and adopt an evaluation procedure for the crack tip opening displacement ($CTOD$) derived directly from experimentally measured records of load vs. crack mouth opening displacement ($CMOD$). The methodology essentially determines the $CTOD$ value from first evaluating the plastic component of J using the plastic work defined by the area under the load vs. $CMOD$ curve and then converting the total J-value into the corresponding value of plastic $CTOD$. The approach has the potential to simplify evaluation of $CTOD$-values while, at the same time, relying on a rigorous energy release rate definition of J for a cracked body yielding the expression (Sarzosa *et al.*, 2015).

$$\delta = \frac{J}{m\sigma_f} \tag{10}$$

in which m represents a proportionality coefficient strongly dependent on the material strain hardening. Here, we note that the material yield stress has been replaced by the flow stress, $\sigma_f = (\sigma_{uts} + \sigma_{ys})/2$ in which σ_{uts} denotes the tensile strength, to incorporate the effects of strain hardening on the J *vs* $CTOD$ relation. Sarzosa *et al.* (2015) provide accurate relationships between J and $CTOD$ described by the dimensionless parameter m for use in testing protocols for toughness measurements. For sidegrooved specimens and using a simple power-hardening model to characterize the uniaxial true stress ($\bar{\sigma}$) *vs.* logarithmic strain ($\bar{\varepsilon}$) in the form

$$\frac{\bar{\varepsilon}}{\varepsilon_{ys}} = \frac{\bar{\sigma}}{\sigma_{ys}}, \varepsilon \leq \varepsilon_{ys} \; ; \; \frac{\bar{\varepsilon}}{\varepsilon_{ys}} = \left(\frac{\bar{\sigma}}{\sigma_{ys}}\right)^n, \varepsilon \leq \varepsilon_{ys} \tag{11}$$

where σ_{ys} and ε_{ys} are the reference (yield) stress and strain, and n is the strain hardening exponent, Sarzosa et al. (2015) arrived at a functional dependence of parameter m with crack size, a/W, hardening exponent, n, and side-groove fraction, sg, in the form

$$m_{SG} = 1.1171 - 0.2777(a/W) + 0.2218(a/W)^2 + 3.4824n^{-1} - 0.0012n + 1.6911sg - 1.1942sg^2 \tag{12}$$

which is valid in the range $0.2 \leq a/W \leq 0.7$, $5 \leq n \leq 20$ and $0 < sg < 0.2$ with the subscript SG corresponding to side-grooved geometry. Here, we note that the side-groove fraction in the above expression is defined as $sg = (B_N/B)$.

Figure 6 recasts the ductile fracture response for the tested girth weld in terms of $CTOD$. Because of the essentially linear relationship between J and $CTOD$ defined by Eq. (10), it is clear that Fig. 7 reproduces the very same features already discussed before. For amounts of stable crack growth of ≈ 1mm, the $CTOD$ -value is in the range of 0.40 ∼ 0.45mm.

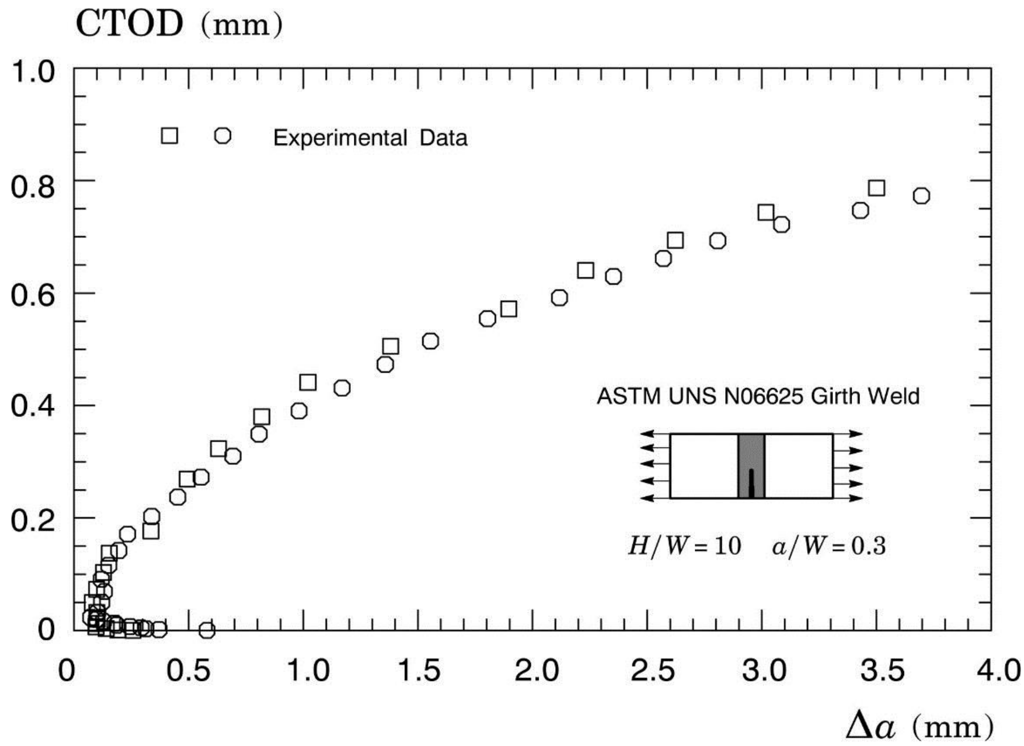

Figure 6: $CTOD$ -resistance curves including crack growth correction for the tested clamped SE(T) specimens with a/W = 0.3 and H/W= 10.

A number of recent procedures, including BS 8571 (British Institution, 2014), adopt a simpler extension of the plastic hinge concept to evaluate the $CTOD$ in clamped SE(T) specimens, which is based on a double clip-gage arrangement. Here, by measuring the crack opening displacements (COD) at two different locations on a straight line passing through the crack flank of the specimen and assuming rigid body rotation, a geometrical relationship between the $CTOD$ for a growing crack and both measured COD -values is obtained. Numerical analyses conducted by Sarzosa *et al*. (2015) show that the $CTOD$ -values derived from the double clip-gage method agree well with the corresponding $CTOD$ -values computed for a growing crack derived from Eq. (10). Unfortunately, since no experimental measurements were made for the $CTOD$ in these two tested specimens, the present results do not allow a direct comparison between both definitions for the $CTOD$.

5. CONCLUDING REMARKS

This study presents an exploratory experimental investigation of the crack growth resistance properties for the girth weld of an API 5L Grade X65 internally clad with a nickel-chromium corrosion resistant alloy (CRA) of ASTM UNS N06625 Alloy 625. Testing of the pipeline girth welds employed side-grooved, clamped SE(T) specimens with a weld centerline notch to determine the crack growth resistance curves based upon the unloading compliance (UC) method using a single specimen technique. The experiments described provide support to use experimentally measured load-displacement data to describe ductile tearing properties for dissimilar girth weld materials. Although the UC procedure underestimated the measured crack extension for one of the tested specimens, our preliminary results demonstrate the capability of the methodology in describing crack growth resistance behavior which serves as a basis for ductile tearing assessments in ECA procedures applicable to clad pipeline girth welds and similar structural components. Further work is in progress to improve the procedure for crack length estimates and crack length measurements, including the potential effects of weld strength undermatch and the clad layer on experimental measurements of the fracture resistance data.

6. ACKNOWLEDGEMENTS

This investigation is supported by the Brazilian State Oil Company (PETROBRAS). Additional support is also provided by the Brazilian Council for Scientific and Technological Development (CNPq) through Grants 306193/2013− 2 and 456222/2013− 8. The authors also acknowledge the useful discussions and contributions of Eduardo Hippert (Petrobras).

7. REFERENCES

American Petroleum Institute, 2007. Fitness-for-service, API RP- 579-1 / ASME FFS-1.

American Society for Testing and Materials, 2009. Standard specification for Nickel-Chromium-Molybdenum-Columbium alloy (UNS N06625) and Nickel-Chromium-Molybdenum-Silicon alloy (UNS N06219) plate, sheet, and strip, ASTM B443-00.

American Society for Testing and Materials, 2011a. Standard specification for Nickel-Chromium-Molybdenum Columbium alloys (UNS N06625 and UNS N06852) and Nickel-Chromium-Molybdenum-Silicon Alloy (UNS N06219) pipe and tube, ASTM B444-06.

American Society for Testing and Materials, 2011b. Standard test method for measurement of fracture toughness, ASTM E1820- 2011.

American Society of Mechanical Engineers, 2009. Boiler and Pressure Vessel Code, Section IX, Welding and Brazing Qualifications.

Anderson, T. L., 2005. Fracture Mechanics: Fundaments and Applications - 3rd Edition. CRC Press, Boca Raton, FL.

British Institution, 2014. Method of test for determination of fracture toughness in metallic materials using single edge notched tension (sent) specimens, BS8571.

Burdekin, F. M., Dawes, M. G., 1966. The crack opening displacement approach to fracture mechanics in yielding materials. Journal of Strain Analysis 1, 144–153.

Cravero, S., Ruggieri, C., 2005. Correlation of fracture behavior in high pressure pipelines with axial flaws using constraint designed test specimens - Part I: Plane-strain analyses. Engineering Fracture Mechanics 72, 1344–1360.

Cravero, S., Ruggieri, C., 2007a. Estimation procedure of *J*resistance curves for SE(T) fracture specimens using unloading compliance. Engineering Fracture Mechanics 74, 2735–2757.

Cravero, S., Ruggieri, C., 2007b. Further developments in *J* evaluation procedure for growing cracks based on LLD and CMOD data. International Journal of Fracture 148, 347–400.

Drexler, E., Wang, Y.-Y., Sowards, J. W., Dvorak, M. D., 2010. SE(T) testing of pipeline welds. In: 8th International Pipeline Conference (IPC). Calgary, Canada.

Harrison, J. D., Dawes, M. G., Archer, G. L., Kamath, M. S., 1979. The COD approach and its application to welded structures. In: Landes, J. D., Begley, J. A., Clarke, G. A. (Eds.), Elastic-Plastic Fracture. ASTM STP 668. American Society for Testing and Materials, Philadelphia, pp. 606–631.

Hutchinson, J. W., 1983. Fundamentals of the phenomenological theory of nonlinear fracture mechanics. Journal of Applied Mechanics 50, 1042–1051.

Joyce, J. A., Hackett, E. M., Roe, C., 1993. Effects of crack depth and mode loading on the *J*-*R* curve behavior of a high strength steel. In: Underwood, J. H., Schwalbe, K.-H., Dodds, R. H. (Eds.), Constraint Effects in Fracture. ASTM STP 1171. American Society for Testing and Materials, Philadelphia, pp. 239–263.

Joyce, J. A., Link, R. E., 1995. Effects of constraint on upper shelf fracture toughness. In: Reuter, W. G., Underwood, J. H., Newman, J. (Eds.), Fracture Mechanics. ASTM STP 1256. American Society for Testing and Materials, Philadelphia, pp. 142– 177.

Kanninen, M. F., Popelar, C. H., 1985. Advanced Fracture Mechanics. Oxford University Press, New York.

Mathias, L. L. S., Sarzosa, D. F. B., Ruggieri, C., 2013. Effects of specimen geometry and loading mode on crack growth resistance curves of a high-strength pipeline girth weld. International Journal of Pressure Vessels and Piping 111-112, 106–119.

Nyhus, B., Polanco, M., Ørjasæter, O., 2003. SENT specimens as an alternative to SENB specimens for fracture mechanics testing of pipelines. In: 22nd International Conference on Ocean, Offshore and Arctic Engineering (OMAE). Vancouver, Canada.

Park, D. Y., Tyson, W. R., Gianetto, J. A., Shen, G., Eagleson, R. S., 2010. Evaluation of fracture toughness of X100 pipe steel using SE(B) and clamped SE(T) single specimens. In: 8th International Pipeline Conference (IPC). Calgary, Canada.

Ruggieri, C., Hippert, E., 2015. Test procedure for fracture resistance characterization of pipeline steels and pipeline girth welds using single-edge notched tension (SENT) specimens. Tech. rep., University of São Paulo.

Sarzosa, D. F. B., Souza, R. F., Ruggieri, C., 2015. *J*-CTOD relations in clamped SE(T) fracture specimens including 3-D stationary and growth analysis. Engineering Fracture Mechanics 147, 331–354.

Shen, G., Bouchard, R., Gianetto, J. A., Tyson, W. R., 2008. Fracture toughness evaluation of high-strength steel pipe. In: ASME PVP 2008 Pressure Vessel and Piping Division Conference. American Society of Mechanical Engineers, Chicago, IL.

Shen, G., Gianetto, J. A., Tyson, W. R., 2009. Measurements of $J - R$ curves using single specimen technique on clamped SE(T) specimens. In: 19th International Offshore and Polar Engineering Conference (ISOPE). Osaka, Japan.

Shen, G., Tyson, W. R., 2009a. Crack size evaluation using unloading compliance in single-specimen single-edge notched tension fracture toughness testing. Journal of Testing and Evaluation 37 (4), JTE102368.

Shen, G., Tyson, W. R., 2009b. Evaluation of CTOD from *J*-integral for SE(T) specimens. In: Pipeline Technology Conference (PTC 2009). Ostend, Belgium.

Silva, L. A. L., Cravero, S., Ruggieri, C., 2006. Correlation of fracture behavior in high pressure pipelines with axial flaws using constraint designed test specimens - Part II: 3-D effects on constraint. Engineering Fracture Mechanics 76, 2123–2138.

Tang, H., Macia, M., Minnaar, K., Gioielli, P., Kibey, S., Fairchild, D., 2010. Development of the SENT test for strainbased design of welded pipelines. In: 8th International Pipeline Conference (IPC). Calgary, Canada.

Wang, E., Zhou, W., Shen, G., Duan, D., 2012. An experimental study on *J* (CTOD)-*R* curves of single edge tension specimens for X80 steel. In: 9th International Pipeline Conference (IPC). Calgary, Canada.

Zhu, X. K., Leis, B. N., Joyce, J. A., 2008. Experimental estimation of *J-R* curves from load-CMOD record for SE(B) specimens. Journal of ASTM International 5 (5), JAI101532.

Zhu, X. K.; Joyce, J., 2007. A. Review of fracture toughness (G, K, J, CTOD, CTOA) testing and standardization. Engineering fracture mechanics 85, 1 – 46.

Zhu, X. K., McGaughy, T., 2014. A review of fracture toughness testing and evaluation using sent specimens. In: 10th International Pipeline Conference (IPC). Calgary, Canada.

8. RESPONSIBILITY NOTICE

The authors are the only responsible for the printed material included in this paper.